NASA CONTRACTOR
REPORT

NASA CR-1872

RADIATION EFFECTS DESIGN HANDBOOK

Section 6. Solid-State Photodevices

by J. E. Drennan

Prepared by
RADIATION EFFECTS INFORMATION CENTER
BATTELLE MEMORIAL INSTITUTE
Columbus, Ohio 43201
for

NATIONAL AERONAUTICS AND SPACE ADMINISTRATION • WASHINGTON, D. C. • AUGUST 1971

1. Report No.	2. Government Accession No.	3. Recipient's Catalog No.
NASA CR-1872		

4. Title and Subtitle	5. Report Date
RADIATION EFFECTS DESIGN HANDBOOK SECTION 6. SOLID-STATE PHOTODEVICES	August 1971
	6. Performing Organization Code
7. Author(s)	8. Performing Organization Report No.
J. E. Drennan	
	10. Work Unit No.
9. Performing Organization Name and Address	
Radiation Effects Information Center Battelle Memorial Institute Columbus Laboratories Columbus, Ohio 43201	11. Contract or Grant No. NASW-1568
	13. Type of Report and Period Covered
12. Sponsoring Agency Name and Address	Handbook - Several Years
National Aeronautics and Space Administration Washington, D. C. 20546	14. Sponsoring Agency Code

15. Supplementary Notes

16. Abstract

This document summarizes information concerning the effects of radiation on solid-state photodevices, especially solar cells. The forms of radiation include neutrons, protons, electrons, and electromagnetic. Several curves are presented.

17. Key Words (Suggested by Author(s))	18. Distribution Statement
Radiation Effects on Solar Cells, Neutrons, Protons, Electrons, Gamma-Rays	Unclassified - Unlimited

19. Security Classif. (of this report)	20. Security Classif. (of this page)	21. No. of Pages	22. Price*
Unclassified	Unclassified	34	$3.00

*For sale by the National Technical Information Service, Springfield, Virginia 22151

ACKNOWLEDGMENTS

The Radiation Effects Information Center owes thanks to several individuals for their comments and suggestions during the preparation of this document. The effort was monitored and funded by the Space Vehicles Division and the Power and Electric Propulsion Division of the Office of Advanced Research and Technology, NASA Headquarters, Washington, D. C., and the AEC-NASA Space Nuclear Propulsion Office, Germantown, Maryland. Also, we are indebted to the following for their technical review and valuable comments on this section:

Dr. B. Anspaugh, Jet Propulsion Laboratory

Mr. S. Manson, NASA Headquarters

Mr. D. J. Miller, Space Nuclear Systems Office

Mr. A. Reetz, Jr., NASA Headquarters

Dr. J. J. Singh, NASA-Langley Research Center

PREFACE

This document is the sixth section of a Radiation Effects Design Handbook designed to aid engineers in the design of equipment for operation in the radiation environments to be found in space, be they natural or artificial. This Handbook will provide the general background and information necessary to enable the designers to choose suitable types of materials or classes of devices.

Other sections of the Handbook will discuss such subjects as transistors, thermal-control coatings, structural metals, and interactions of radiation, electrical insulating materials, and capacitors.

TABLE OF CONTENTS

SECTION 6. SOLID-STATE PHOTODEVICES

INTRODUCTION

A photodevice, as the name implies, is intended to provide an electrical response to incident photons of radiation. This section will consider two basic types of photocells in use: photovoltaic and photoconductive "bulk effect".

The photovoltaic cell generates a voltage across a P/N or N/P junction as a function of the photons impinging on it. Silicon, gallium arsenide, cadmium sulfide, and selenium are normally used to make cells of this class. This class of cells is the only self-generating type requiring no external power supply. Solar cells are photovoltaic cells employed to generate electric power from incident solar photon radiation.

Photoconductive cells employing the bulk effect are normally made of cadmium sulfide (CdS) or cadmium selenide (CdSe) and have no junction. The entire layer of material changes in resistance under illumination. This response is analogous to a thermistor except that heat is replaced by light. The photoconductive cell decreases in resistance as the light level increases. The absolute value of resistance of a particular cell at a specific light level depends on the photosensitive material employed, cell size, electrode geometry, and the spectral composition of the incident light.

Although some overlap is possible, generally the prime usage of photovoltaic cells is in solar cells intended to convert solar energy to useful electric power. The photoconductive cells primarily are used in applications that are now combined in the field of optoelectronics. The field of optoelectronics generally involves a combination of solid-state technology and light measurement. Hence, the field of optoelectronics would include the detection and/or measurement of radiation energy from infrared through visible and ultraviolet and the use of these radiation wavelengths for control or other electronic purposes. Both classes of cells may be used for detection and/or measurement of nuclear radiation.

RADIATION EFFECTS ON PHOTOVOLTAIC DEVICES

Solar Cells

The solar cell is one of the most critical components in some satellite systems where it constitutes the primary source of electric power to operate the electronic systems. In this application, the solar cells are normally located outside the space-vehicle skin where they are exposed to the direct space-radiation environment modified only by relatively thin, optically transparent covers. The optical properties of cover materials employed to protect the basic solar cell from the space environment are degraded by exposure to radiation, and the cell itself is degraded by radiation penetrating the protective cover.

The basic kinds of solar cells available for engineering use include various kinds of silicon P/N and N/P cells, gallium-arsenide cells, and cadmium-sulfide cells. The state-of-the-art in efficiencies of gallium-arsenide and cadmium-sulfide cells (8 to 9 percent and 2 to 3 percent, respectively) restrict the choice for practical systems to the more efficient silicon cells at present, even though both of the compound semiconductor cell types appear to be more resistant to radiation damage than are the silicon cells.

Silicon Solar Cells

The information available about radiation effects on silicon solar cells indicates in general the following:

(1) In the range from 15 to 65 percent electron-induced degradation (increase) in short-circuit current, I_{SC} (and, for practical purposes, that for maximum available power, $P_{(max)}$) degradation in silicon solar cells is independent of the energy of the bombarding electron, depending only on the optical absorption characteristics of light in silicon and, thus, on the illumination source. The respective rates for radiation-induced I_{SC} and $P_{(max)}$ degradation in silicon cells of all types under solar illumination are approximately 15 and 20 percent per decade of radiation fluence above the threshold fluence.

(2) A similar statement can be made for gallium-arsenide cells, except that the degradation rate also appears to be independent of illumination source. The typical degradation rate for I_{SC} in gallium-arsenide cells is 45 to 50 percent per decade of radiation fluence.

(3) The fluence threshold for silicon solar-cell damage and the critical fluence, Φ_c*, depend upon cell type (N/P, P/N), base resistivity, and the type and energy of the bombarding particle.

(4) The energy dependence of proton-radiation damage in silicon solar cells is found to be approximately inversely proportional to proton energy over the range of proton energies from 6.7 MeV to about 100 MeV. At energies above 100 MeV, the damage dependence upon further increases in proton energy appears to become gradually less, theoretically approaching a plateau independent of proton energy.

(5) For silicon cells, the short-circuit current is little affected by low-energy protons ($E < 1$ MeV), but the open-circuit voltage decreases more rapidly under low-energy-proton bombardment than for higher energy irradiations.

(6) The sensitivity to radiation-induced degradation of silicon solar cells is significantly greater for P/N than for N/P cells.

(7) Silicon solar cells containing an additional lithium dopant generally can perform satisfactorily at higher radiation fluences than comparable cells that do not contain the lithium dopant.

In the normal space application for solar cells, the cells are either exposed directly to the space radiation or else a thin, transparent protective cover is employed. Such a cover is usually of such a thickness to protect against proton energies up to 20 MeV. In either case, electron and

*Φ_c is defined as the value of radiation fluence producing 20 percent degradation in maximum available power $P_{(max)}$; that is, at Φ_c the ratio $P_{(max)}/P_{(max)_0} = 0.8$ or in other words critical fluence Φ_c, can be defined as the value of fluence for which $P_{(max)}$ is 80 percent of its preirradiation value. Φ_c is about one decade greater than the threshold fluence where the first significant bulk radiation effects should be observed and has the advantage of being experimentally measurable whereas the threshold fluence is normally masked by surface effects.

proton bombardment are the major factors causing solar-cell degradation and most of the available radiation-effects data pertain to these radiation particles. However, if the environment contains an appreciable neutron component, than the neutron fluence also will contribute to the solar-cell degradation.

To assist the electronic-design engineer during early design phases, the information in the REIC files has been employed as the basis for preparation of the performance envelopes in Figures 1 through 16.* In these figures the ratio of maximum available power to the initial value of maximum available power, $P_{(max)}/P_{(max)o}$, is plotted as a function of radiation fluence.** The envelopes presented encompass the data available in the REIC files. Representative data points are plotted within these envelopes.

The intended use of these envelopes is as follows: if the electronic designer finds the radiation fluence of his expected application environment to be outside the appropriate envelope in the low-fluence direction, he should not expect significant radiation-induced degradation of solar cells; however, for an application environment falling within the envelope, radiation-induced degradation of solar-cell performance ranging from mild to severe should be anticipated; finally, if the application environment falls outside the envelope in the high-fluence direction, very severe radiation-induced solar-cell degradation can be expected.

Figures 17 and 18 show the dependence of critical fluence, Φ_c, upon electron energy for five resistivities of N/P and P/N silicon solar cells, respectively. The semiempirical model is as follows:

$$P_{(max)}/P_{(max)_o} = A\,(\log(E))^2 + B\log(E) + C + D\log(\rho) - 0.2\log(\Phi)$$

where

$P_{(max)o}$ = preirradiation value of maximum power

E = electron energy

ρ = solar-cell resistivity

Φ = electron fluence

* Extrapolation of these envelopes outside the range plotted should not be attempted.

** The range of proton energies for which data are plotted is from 0.5 to 20 MeV. The envelopes were generated assuming the degradation rate to be independent of energy over this range. Some of the data spread undoubtedly results because this assumption is not strictly true. However, the available data are not sufficient to provide more accurate envelopes.

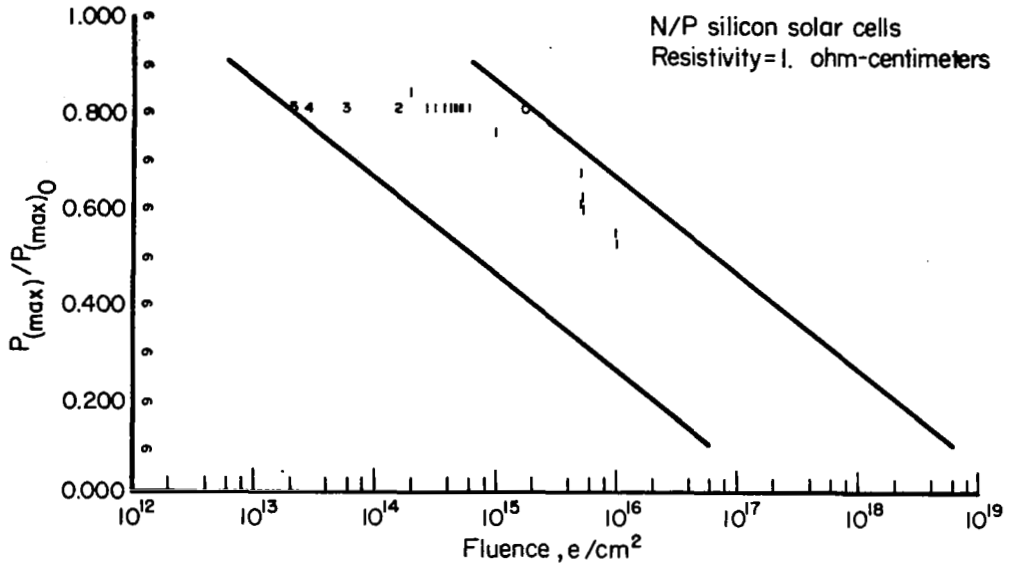

FIGURE 1. $P_{(MAX)}/P_{(MAX)_0}$ VERSUS ELECTRON FLUENCE

22 sets of data.

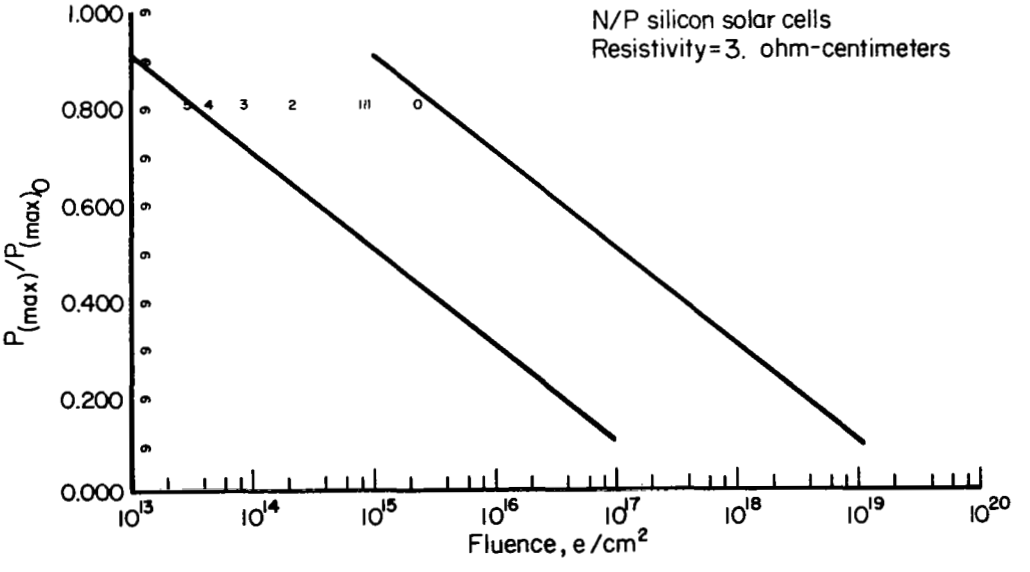

FIGURE 2. $P_{(MAX)}/P_{(MAX)_0}$ VERSUS ELECTRON FLUENCE

8 sets of data.

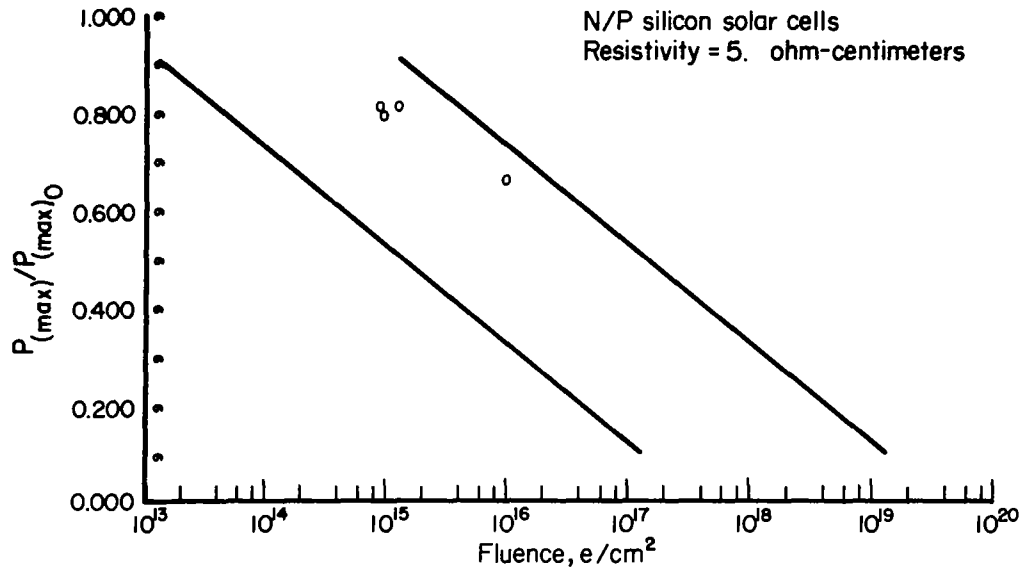

FIGURE 3. $P_{(MAX)}/P_{(MAX)_0}$ VERSUS ELECTRON FLUENCE

4 sets of data.

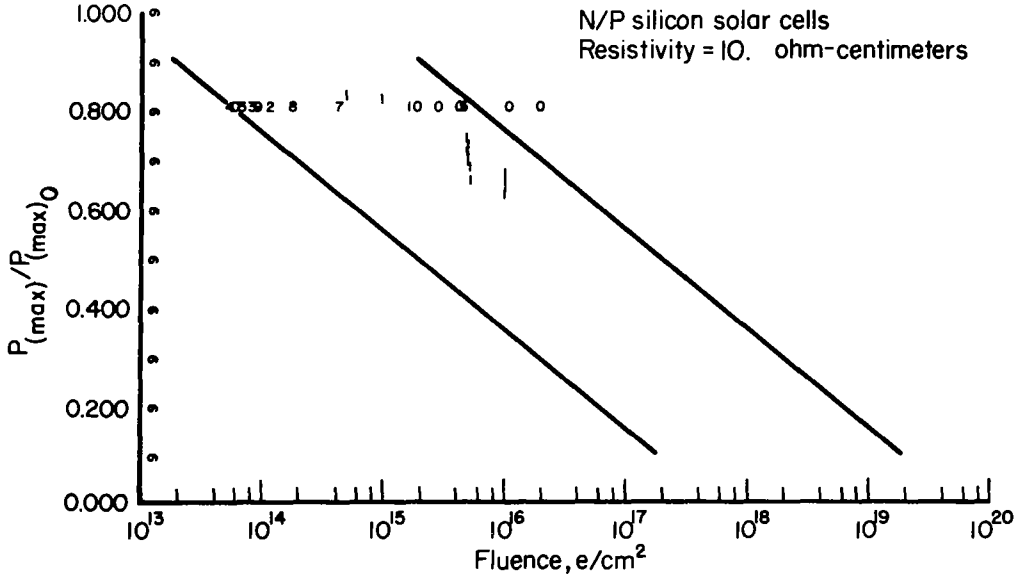

FIGURE 4. $P_{(MAX)}/P_{(MAX)_0}$ VERSUS ELECTRON FLUENCE

32 sets of data.

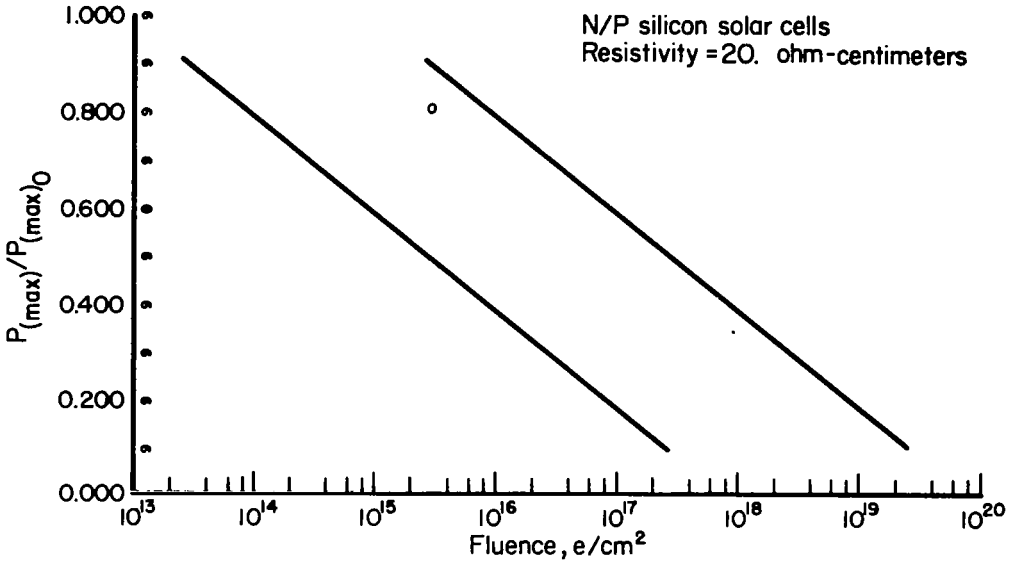

FIGURE 5. $P_{(MAX)}/P_{(MAX)_0}$ VERSUS ELECTRON FLUENCE

1 set of data.

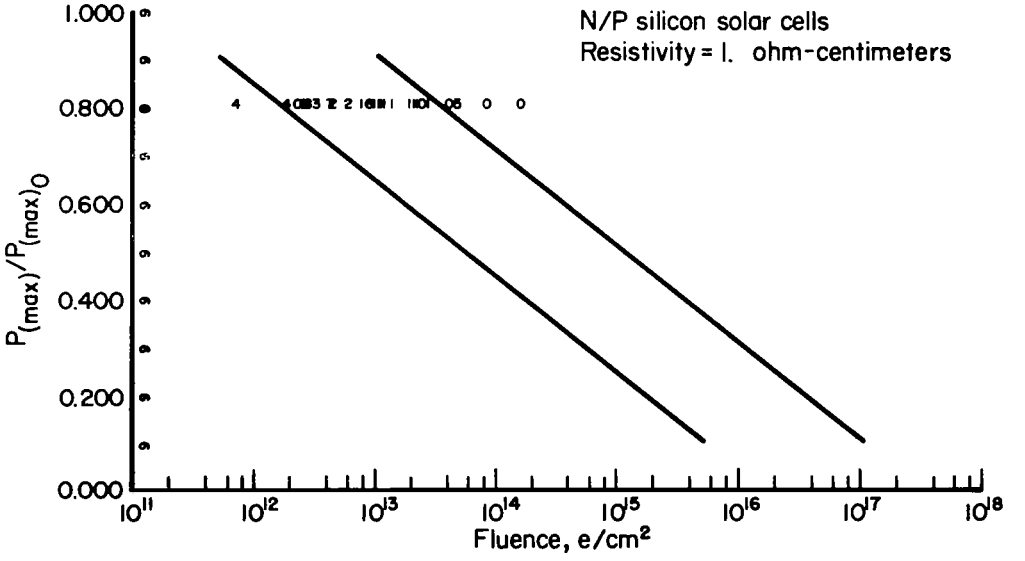

FIGURE 6. $P_{(MAX)}/P_{(MAX)_0}$ VERSUS ELECTRON FLUENCE

21 sets of data.

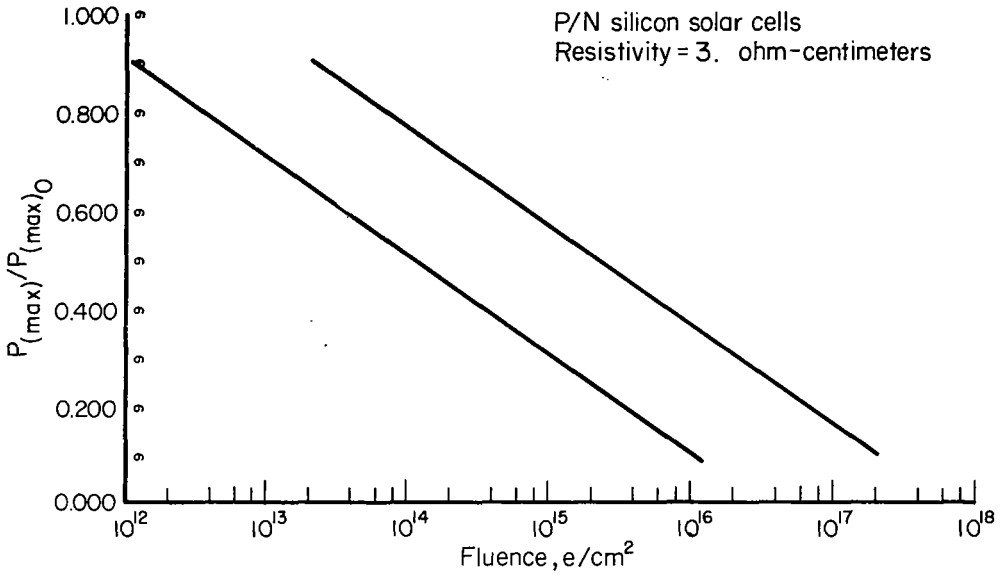

FIGURE 7. $P_{(MAX)}/P_{(MAX)_0}$ VERSUS ELECTRON FLUENCE

0 sets of data.

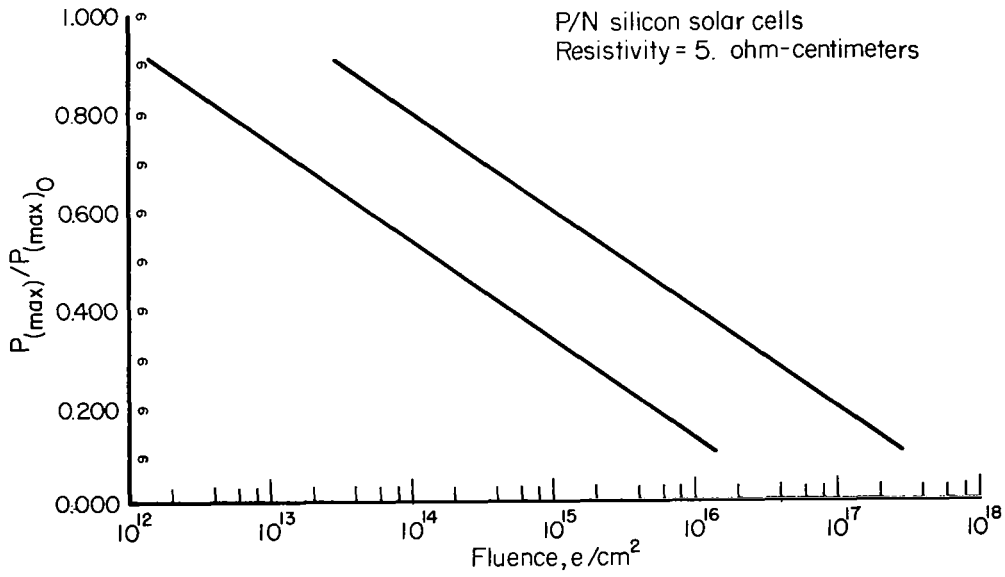

FIGURE 8. $P_{(MAX)}/P_{(MAX)_0}$ VERSUS ELECTRON FLUENCE

0 sets of data.

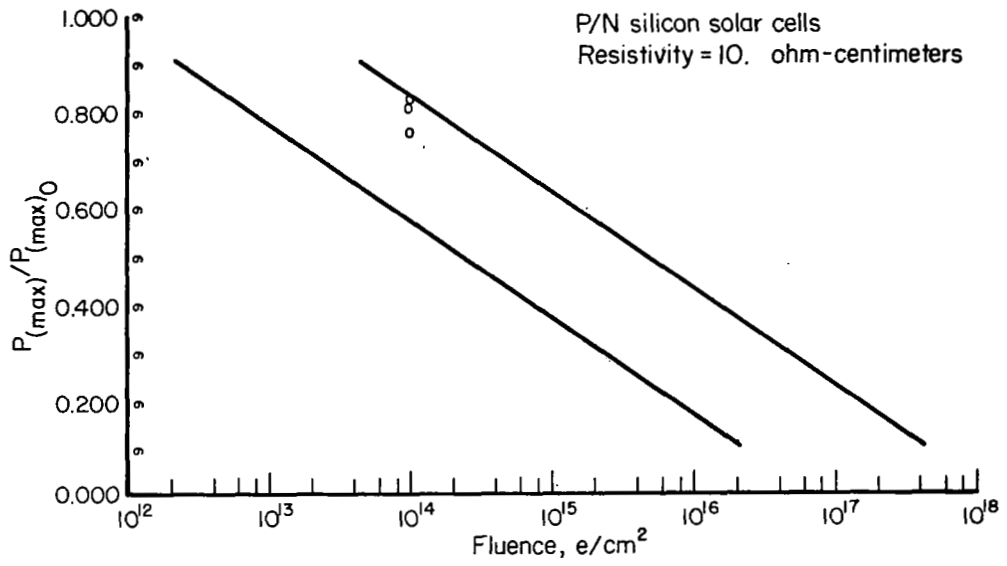

FIGURE 9. $P_{(MAX)}/P_{(MAX)_0}$ VERSUS ELECTRON FLUENCE

3 sets of data.

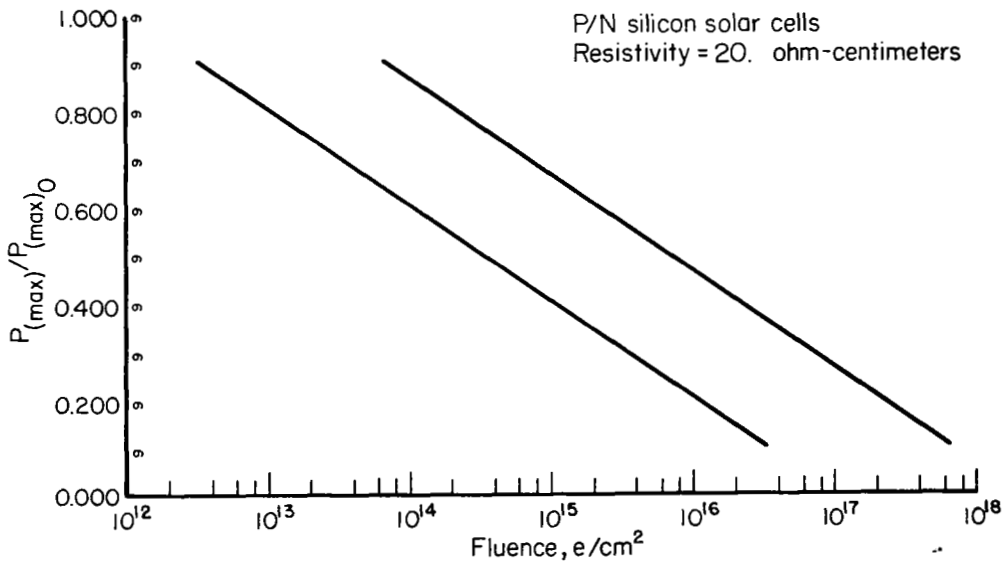

FIGURE 10. $P_{(MAX)}/P_{(MAX)_0}$ VERSUS ELECTRON FLUENCE

0 sets of data.

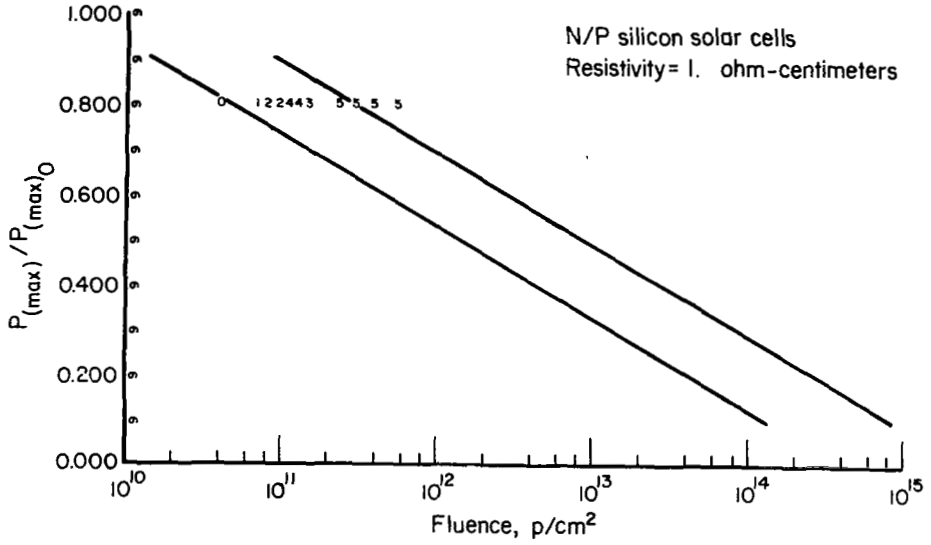

FIGURE 11. $P_{(MAX)}/P_{(MAX)_0}$ VERSUS PROTON FLUENCE (0.5 MEV < E < 20 MEV)

13 sets of data.

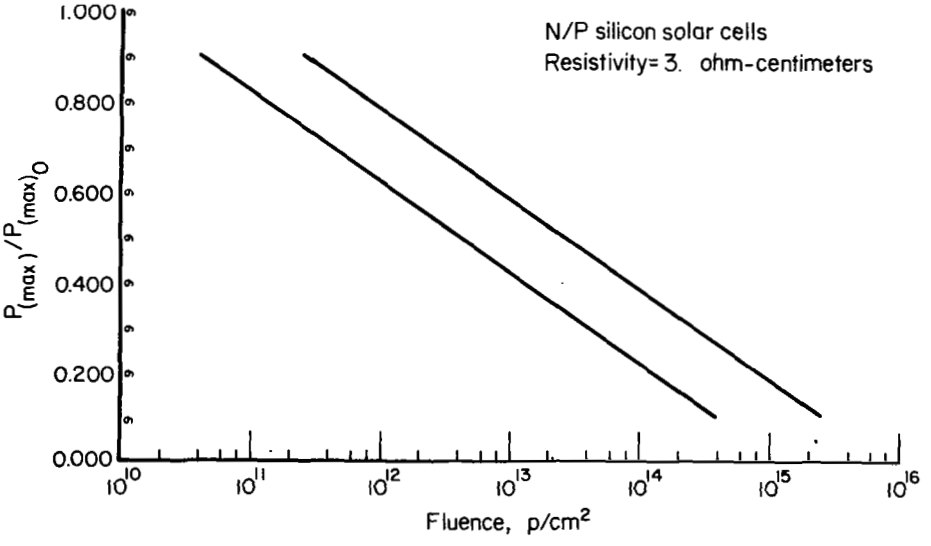

FIGURE 12. $P_{(MAX)}/P_{(MAX)_0}$ VERSUS PROTON FLUENCE (0.5 MEV < E < 20 MEV)

0 sets of data.

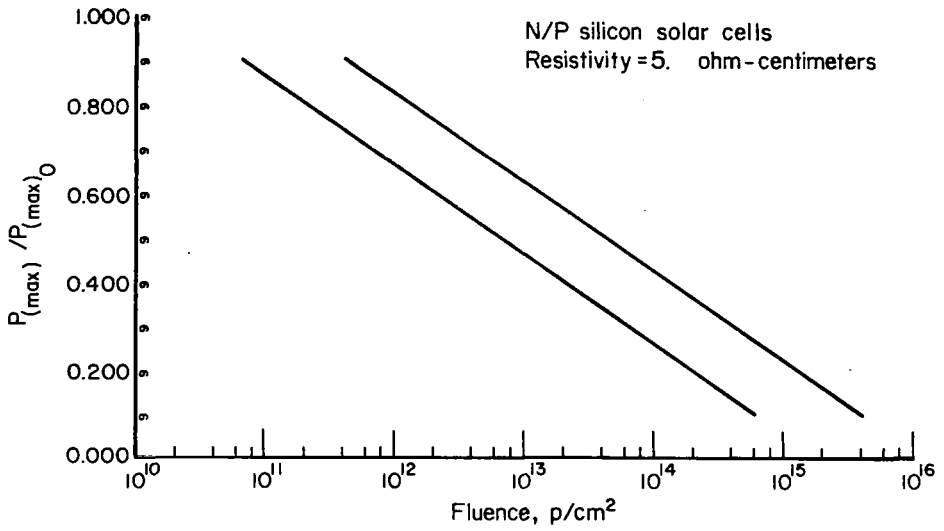

FIGURE 13. $P_{(MAX)}/P_{(MAX)_0}$ VERSUS PROTON FLUENCE (0.5 MEV < E < 20 MEV)

0 sets of data.

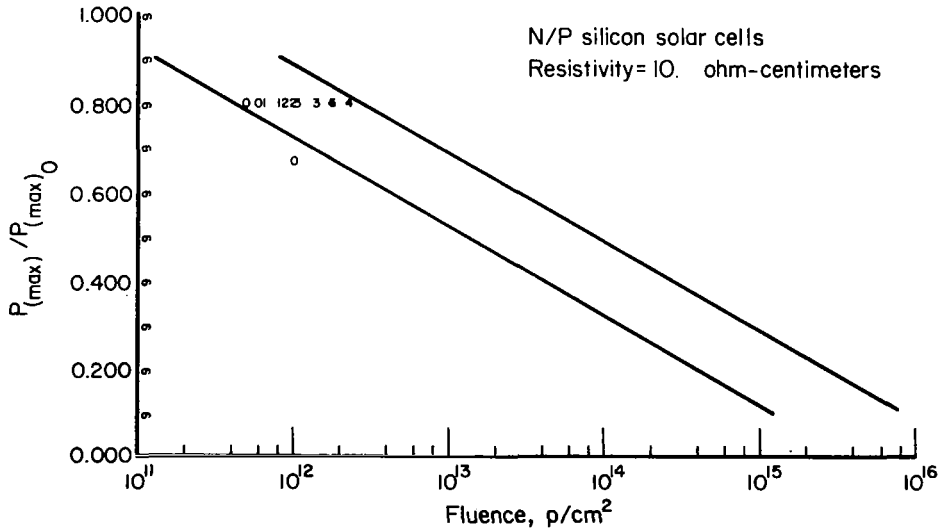

FIGURE 14. $P_{(MAX)}/P_{(MAX)_0}$ VERSUS PROTON FLUENCE (0.5 MEV < E < 20 MEV)

13 sets of data.

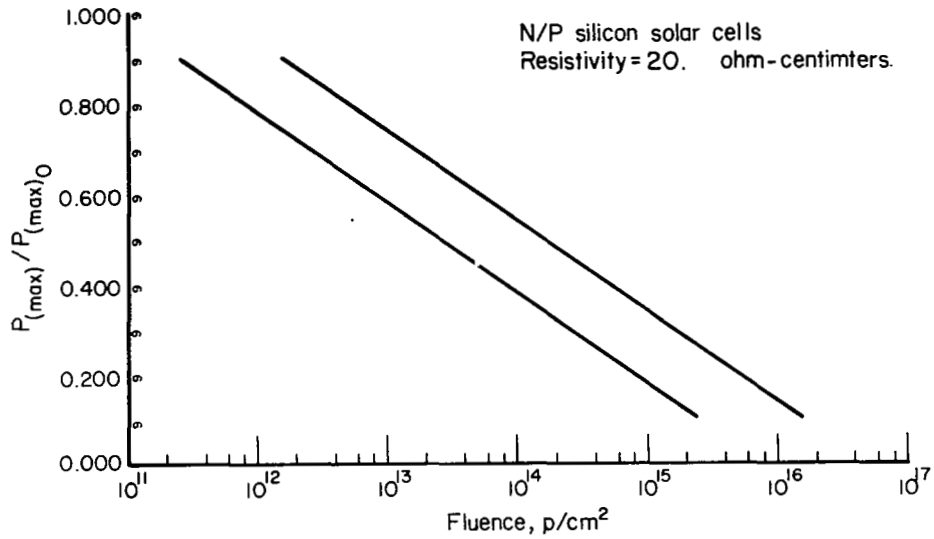

FIGURE 15. $P_{(MAX)}/P_{(MAX)_0}$ VERSUS PROTON FLUENCE (0.5 MEV < E < 20 MEV)

0 sets of data.

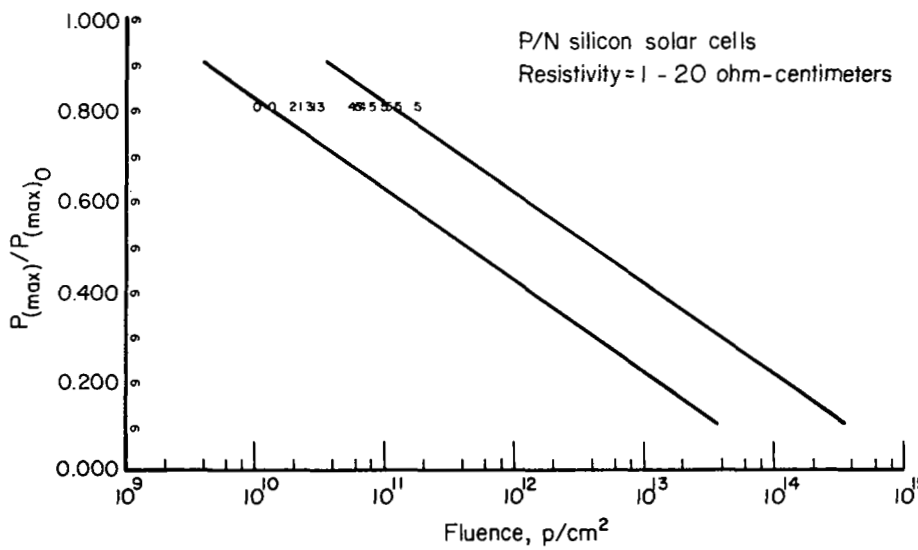

FIGURE 16. $P_{(MAX)}/P_{(MAX)_0}$ VERSUS PROTON FLUENCE (0.5 MEV < E < 20 MEV)

16 sets of data.

was used to generate these curves. The data available in the REIC were fitted to this model by the method of least squares to determine the coefficients given in Table 1.

Figures 19 and 20 show the dependence of Φ_c upon proton energy for five resistivities of N/P silicon solar cells and 1 ohm-centimeter-resistivity P/N silicon solar cells, respectively. The available data for energies above 5 MeV were fitted to the model described earlier except that the value for the coefficient, A, was predetermined to be zero. In the case of the P/N cells, the available data were not sufficient to permit determining a value for D other than zero. The coefficient values determined from the data are listed in Table 1.

TABLE 1. MODEL COEFFICIENTS

Solar Cell Type	A	B	C	D
		Electron Irradiation		
N/P Silicon	0.09839	-1.520	9.325	0.09496
P/N Silicon	0.09545	-1.407	8.425	0.1208
		Proton Irradiation		
N/P Silicon	0.0	0.1232	2.102	0.1926
P/N Silicon	0.0	0.1485	1.822	0.0

The very limited amount of data available for neutron-irradiated solar cells confirm that their behavior under this form of radiation is similar to that produced by electrons and protons although the damage produced is not identical. For N/P silicon solar cells of nominally 5 to 10 ohm-centimeter base resistivity, an average value (subject to considerable variance of critical fluence, $\Phi_c \cong 7 \times 10^{11}$ n/cm^2 (E > 10 keV), has been observed. The effect of changes in neutron energy spectrum has not been documented.

Figure 21 shows the maximum available power ratio, $P_{(max)}/P_{(max)_o}$, versus incremental fluence, $\Delta\Phi$. The incremental fluence is defined as the amount of fluence exceeding the critical fluence value. Thus, Figure 21

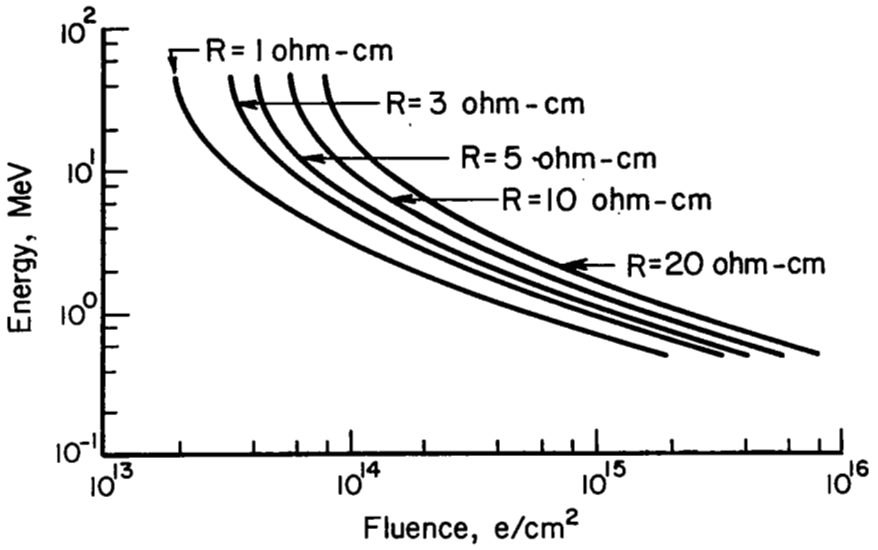

FIGURE 17. CRITICAL FLUENCE VERSUS ELECTRON ENERGY, R=1-20 OHM-CM, N/P

67 sets of data.

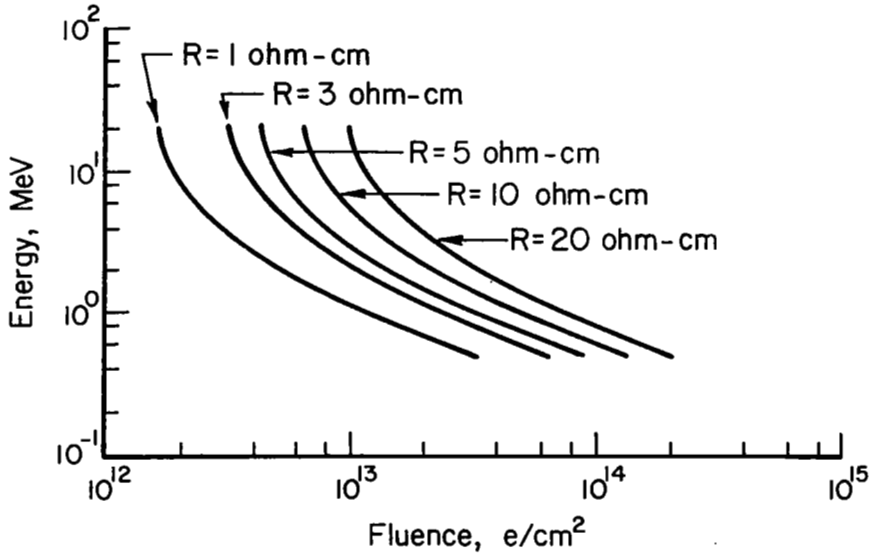

FIGURE 18. CRITICAL FLUENCE VERSUS ELECTRON ENERGY, R=1-20 OHM-CM, P/N

30 sets of data.

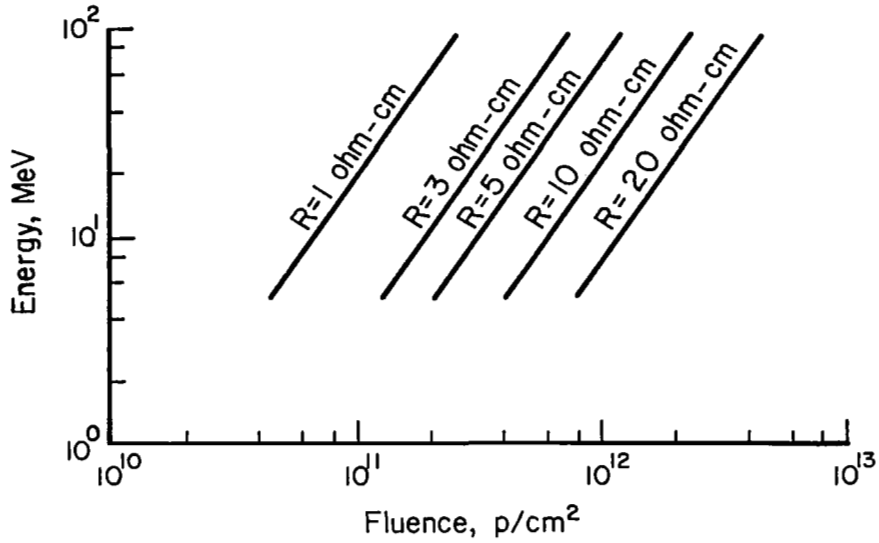

FIGURE 19. CRITICAL FLUENCE VERSUS PROTON ENERGY, R=1-20 OHM-CM, N/P

26 sets of data.

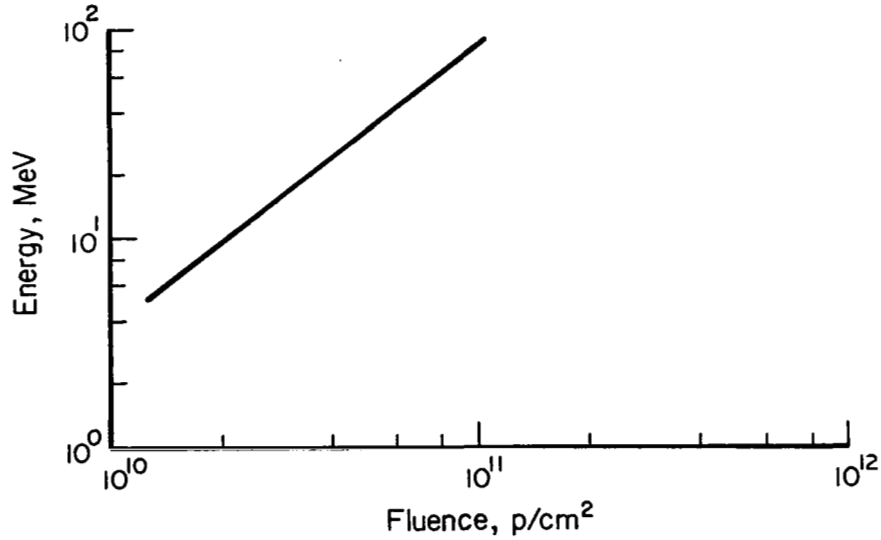

FIGURE 20. CRITICAL FLUENCE VERSUS PROTON ENERGY, R=1 OHM-CM, P/N

16 sets of data.

may be used in conjunction with the neutron critical fluence or with Figure 17, 18, 19, or 20 to predict the typical $P_{(max)}/P_{(max)_o}$ value for a specified solar-cell type, radiation-particle type and energy, and a specified fluence by the following procedure:

(1) Use the critical fluence value for neutron irradiation or determine the appropriate critical fluence value from Figures 17, 18, 19, or 20.

(2) Determine $\Delta\Phi$ by subtracting Φ_c from the specified application fluence. If $\Delta\Phi$ is negative, $P_{(max)}/P_{(max)_o} > 0.8$.

(3) For positive values of $\Delta\Phi$, enter Figure 21 with the value of $\Delta\Phi$ determined in Step (2) and read the corresponding value of typical $P_{(max)}/P_{(max)_o}$.

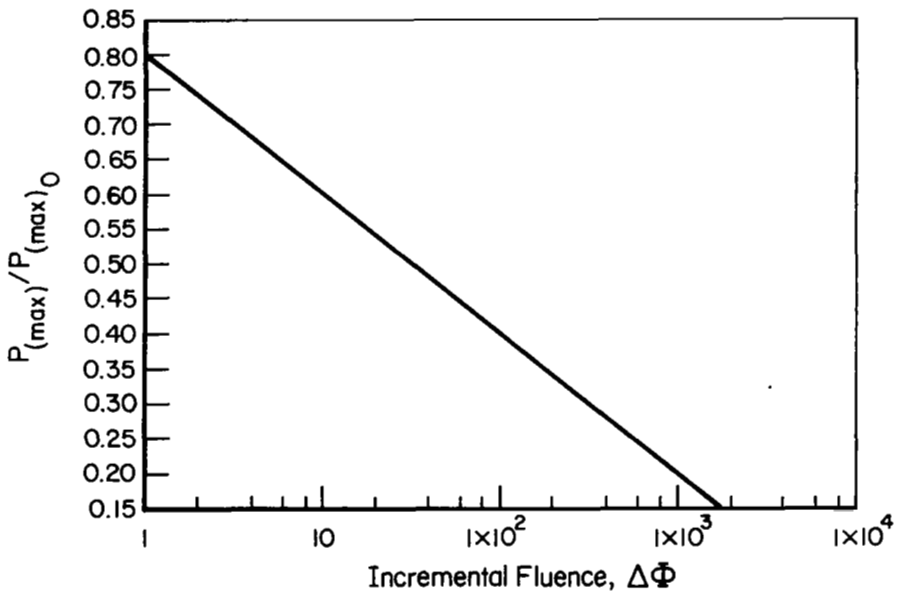

FIGURE 21. DEGRADATION OF $P_{(MAX)}/P_{(MAX)_o}$ AS A FUNCTION OF FLUENCE ABOVE THE CRITICAL FLUENCE Φ_c

The user is cautioned not to attempt extrapolation of these curves outside the plotted range.

The model also can be used to predict a value for $P_{(max)}/P_{(max)_o}$ for given conditions. However, the model is not valid for electron energies outside the range from 4 keV to 40 MeV or for proton energies outside the range from 5 to 100 MeV. The data available for proton energies less than 5 MeV show a high dependence upon cell structure, the type and thickness of cover materials and adhesives, and other manufacturing variables. The variability of these data is too great to permit the development of simple predictive relationships for radiation effects.

In addition to the N/P or P/N silicon solar cells with fixed base resistivities, drift-field or graded-base solar cells have been produced that exhibit improved radiation tolerance. The radiation-induced degradation pattern for these cells is about the same as for conventional N/P solar cells ($P_{(max)}/P_{(max)_o}$ degrades about 20 percent per decade increase in fluence above the threshold fluence). However, the threshold fluence and critical fluence are a factor of three or more greater than those for conventional N/P cells. This is illustrated by the comparison of radiation-induced change of $P_{(max)}/P_{(max)_o}$ for N/P graded-base cells and conventional cells of various resitivities shown in Figure 22.

Another approach to increasing the radiation tolerance of silicon solar cells is the addition of lithium as a dopant in the semiconductor. The lithium diffuses to damage centers produced when high-energy particles bombard the silicon. The action of the lithium diffusion is to effect a recovery of the radiation-degraded electrical properties of the semiconductor. The end result is similar to the result of annealing radiation damage but occurs with reasonable rates at much lower temperatures than the usual annealing temperatures. Thus, though high flux radiation will degrade the lithium-doped solar cells, the properties will recover in hours or days to nearly their original condition even at room temperature.

Much effort has been expended since about 1967 to establish the optimum design for lithium-doped silicon solar cells. A number of trade-offs are required to obtain acceptable electrical properties and avoid re-degradation. The information available in the REIC indicates that the lithium-doped devices are still mainly experimental. No information is available about the performance of "production" devices. However, this technology seems to hold considerable promise for the immediate future.

Thin-Film Cadmium Sulfide Solar Cells

The initial efficiency of CdS solar cells (2 to 3 percent) averages 20 percent or less of the typical silicon solar-cell efficiency. However, available data show that Φ_c for these cells exceeds 10^{17} e/cm^2 for electron energies ranging from 60 keV to 2.5 MeV and exceeds 3×10^{14} p/cm^2 for proton energies ranging from 2 to 10 MeV. Thus, the actual power output of the CdS solar cells at a proton fluence of 4×10^{12} p/cm^2 (E = 1.8 - 3.0 MeV) may be almost the same as that of 1-ohm-centimeter-resistivity N/P silicon solar cells after this exposure. The CdS cells will not have degraded significantly, while the Si cells will be severely degraded. A similar comparison is possible for 1-ohm-centimeter-resistivity P/N Si cells and CdS cells at a 1-MeV electron fluence of 5×10^{15} e/cm^2. It is seen that, even though the CdS cell output for radiation fluences less than these values is relatively constant, this output will be less than that for a silicon cell of comparable area. The CdS cells would have an output advantage only at fluences higher than these.

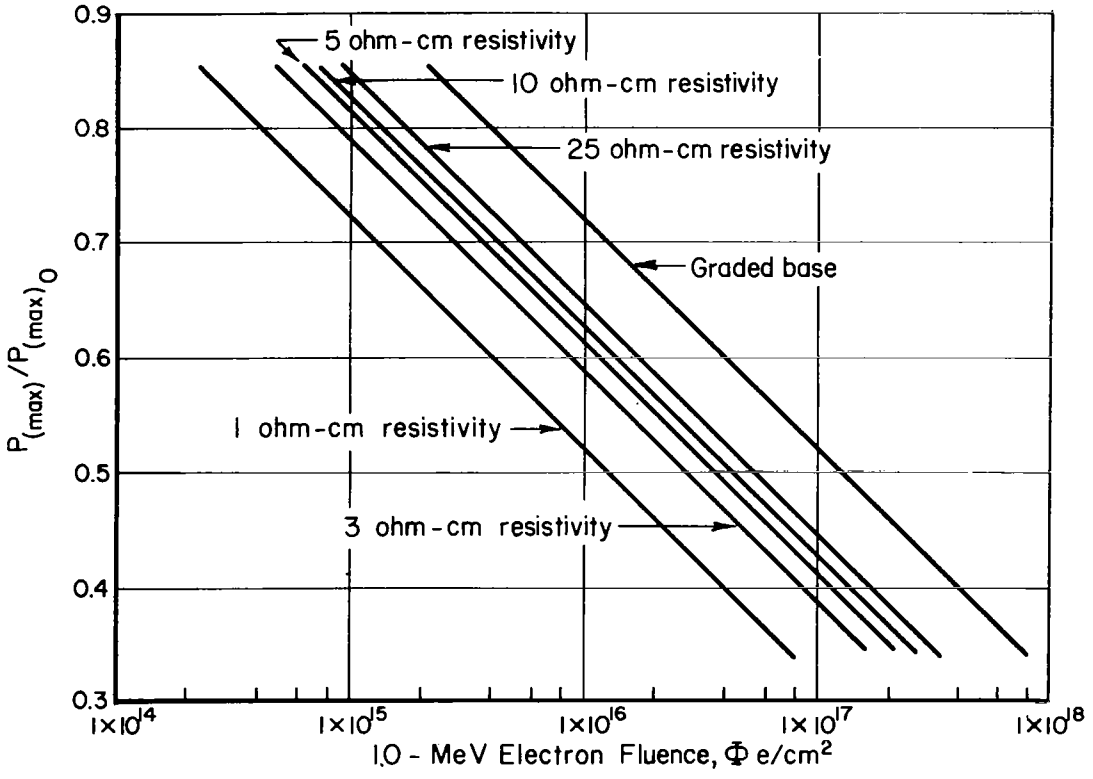

FIGURE 22. N/P SILICON SOLAR-CELL MAXIMUM AVAILABLE POWER RATIO VERSUS 1.0-MEV ELECTRON FLUENCE FOR VARIOUS CELL RESISTIVITIES

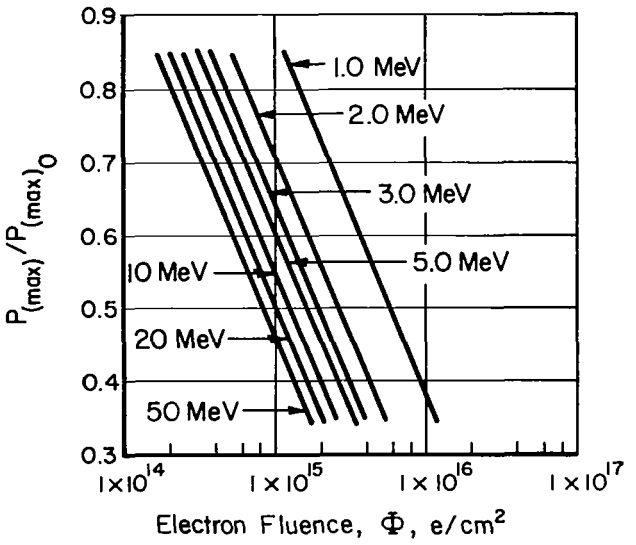

FIGURE 23. $P_{(MAX)}/P_{(MAX)_0}$ VERSUS ELECTRON FLUENCE FOR GaAs SOLAR CELLS

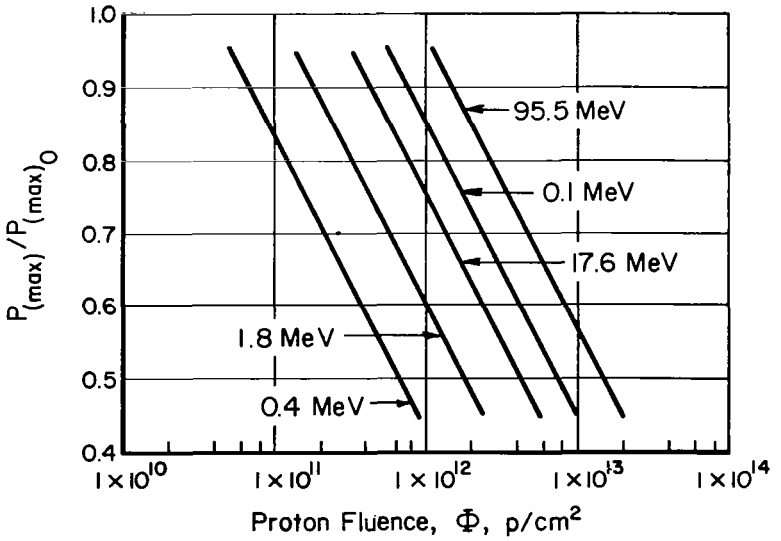

FIGURE 24. $P_{(MAX)}/P_{(MAX)_0}$ VERSUS PROTON FLUENCE FOR GaAs SOLAR CELLS

Gallium Arsenide Solar Cells

Figure 23 shows $P_{(max)}/P_{(max)_o}$ for gallium arsenide solar cells as a function of electron fluence for energies ranging from 1 to 50 MeV. Figure 24 shows $P_{(max)}/P_{(max)_o}$ as a function of proton fluence for energies ranging from 0.1 to 95.5 MeV. The available GaAs solar-cell data are not sufficient to permit a more complete analysis.

Solar-Cell Cover Glasses and Adhesives

The preceding discussion has treated the solar cell as a device without considering whether or not the semiconductor element is protected by a transparent shield. Experimental data have shown that the degradation of the semiconductor element of the solar cells resulting from space radiation can be substantially reduced if the solar cells are protected with a transparent shield. However, the use of such a shield may present other problems, such as the effects of radiation on the light transmissivity of the shield material and adhesive. Also, the protected-solar-cell efficiency may initially be less than that for an unprotected cell because some light energy may be lost in the shield material and adhesive. A variety of glasses, fused quartz and silicas, sapphire, and plastic materials, as well as various adhesives have been studied for a range of electron and proton energies and exposure. The reader is referred to the "Handbook of Space-Radiation Effects on Solar-Cell Power Systems"* for a more detailed discussion of these subjects.

Some generalized information on space radiation effects on transparent materials and adhesives is presented in Tables 2, 3, and 4.

* See, in Bibliography, Cook, W. C., "Handbook of Space-Radiation Effects on Solar-Cell Power Systems", 1963.

TABLE 2. EFFECTS OF ELECTRONS AND PROTONS ON OPTICAL CHARACTERISTICS OF SOLAR-CELL COVER MATERIALS

Material Description	Percent Change in Transmittance Wavelength, μ 0.5	0.6	0.7
(A) 1-MeV Electrons (Total Dose: 10^{16} e cm^{-2})			
(1) Microsheet (6-mil) Corning 0211	5.6	3.3	2.2
(2) Same as (1) + A-R coating + "blue" filter	7.3	5.1	4.2
(3) Same as (1) + A-R coating + "blue-red" filter	9.9	8.6	6.9
(4) 3 mil microsheet + A-R coating + "blue" filter	3.7	2.1	
(5) Fused silica (66 mil) Corning 7940	1.7	2.2	1.1
(6) Fused silica-Corning 7940 (20 mil) +A-R coating + "blue" filter	1.1	2.2	1.1
(7) Adhesive ES-10 (Spectrolab)	1.7	1.7	1.1
(8) Adhesive 15-E (Furane)	24	13	12
(9) Adhesive DER-332 (LC) (Dow)	8.6	9.1	4.5
(B) 4.6-MeV Protons (Total Dose: 4×10^{11} p cm^{-2})			
(1) Microsheet (6 mil) Corning 0211	3.4	1.1	1.1
(2) Same as (1) + A-R coating + "blue" filter	5.2	2.1	1.1
(3) Fused silica (30 mil) Corning 7940		no change	
(4) Fused silica (20 mil) + A-R coating + "blue filter"		no change	

TABLE 3. EFFECTS OF 1.2-MeV ELECTRON RADIATION ON TRANSPARENT MATERIALS

Manufacturers	Type Number or Trade Name	Sample Thickness, in.	Total Fluence, e cm^{-2}	Decrease in Light Transmission, percent
		Fused Silica		
Corning Glass Works	No. 7940 (UV grade)	1/16, 1/8	2.7×10^{15}	0.0
Corning Glass Works	No. 7940 (Optical grade)	1/8	2.7×10^{15}	
Engelhard Industries, Inc.				
Amersil Quartz Div.	Suprasil II	1/16, 3/32	2.7×10^{15}	0.0
Amersil Quartz Div.	Optical	1/16	2.7×10^{15}	1.8
Amersil Quartz Div.	Homosil	1/16	2.7×10^{15}	2.1
Amersil Quartz Div.	Ultrasil	1/16	2.7×10^{15}	6.4
Amersil Quartz Div.	Infrasil II	1/16	2.7×10^{15}	23.0
Thermal American Fused Quartz Co.	Spectrasil A	1/8	2.7×10^{15}	0.0
General Electric Co.				
Willoughby Quartz Plant	GE 104	3/32	2.7×10^{15}	0.8
Willoughby Quartz Plant	GE 105	3/32	2.7×10^{15}	30.0
Willoughby Quartz Plant	GE 106	3/32	2.7×10^{15}	26.6
Dynasil Corporation	Dynasil Optical Glass	1/8	2.7×10^{15}	0.0
		Other Materials		
Linde Company	Sapphire	0.020	2.7×10^{15}	0.0
Pittsburgh Plate Glass Company	Solex	1/4	2.7×10^{15}	2.7
Corning Glass Works	Vycor	1/4	1.7×10^{15}	58.9
--	Soda lime plate glass	1/4	1.7×10^{15}	26.0

TABLE 4. EFFECTS OF ULTRAVIOLET RADIATION ON SPECTRAL TRANSMITTANCE OF TRANSPARENT ADHESIVES[a, b]

	Percent Change in Transmittance at Indicated Wavelength			
Material Designation	0.5 μ	0.6 μ	0.7 μ	0.8 μ
ES-10 (Spectrolab)	23	13	8.6	6.4
15-E (Epocast)	43	31	27	25

(a) Specimens are 1 to 2-mil-thick films cast between sheets of fused silica, 30-mil base, and 6-mil cover sheet with no cutoff filter to limit the UV reaching the specimen.

(b) Exposure equivalent to 630 hr of space UV.

BIBLIOGRAPHY

Brown, D. M., "Low Energy Proton Damage Effects in Silicon and Gallium Arsenide Solar Cells", NASA, Goddard Space Flight Center, Greenbelt, Maryland, NASA-TM-X-54990, 20 pp, Avail: NASA, N65-16347.

Brucker, G. J., "Action of Lithium in Radiation-Hardened Silicon Solar Cells", Astro Electronics, Princeton, New Jersey, AED-R-3389, NASA-CR-98717, November 15, 1968, Qtly Rpt. No. 2, July 16 – October 15, 1968, NAS5-10239, 81 pp, Avail: NASA, N69-14919 and NTIS.

Brucker, G. J., Faith, T. J., and Holmes-Siedle, A. G., "Action of Lithium in Radiation-Hardened Silicon Solar Cells", RCA, Princeton, New Jersey, AED-R-3440, NASA-CR-103871, April 21, 1969, Final Rpt., April 23, 1968 – April 21, 1969, NAS7-100, 119 pp. Avail: NASA, N69-33590 and NTIS.

Carter, J. R., and Downing, R. G., "Effects of Low Energy Protons and High Energy Electrons on Silicon", TRW Space Technology Laboratories, Redondo Beach, California, NASA-CR-404, March, 1966, NAS5-3805, 50 pp. Avail: NASA, N66-18429.

Cooley, W C., and Janda, R. J., "Handbook of Space-Radiation Effects on Solar-Cell Power Systems", Exotech, Inc., Alexandria, Virginia, NASA-SP-3003, 1963, 107 pp.

Denny, J. M., Downing, R. G., Kirkpatrick, M. E., Simon, G. W., and Van Atta, W. K., "Charged Particle Radiation Damage in Semiconductors, IV: High Energy Proton Radiation Damage in Solar Cells", Space Technology Labs., Inc., Redondo Beach, California, MR-27, STL-8653-6017-KU-000, January 20, 1963, NAS5-1851, 57 pp.

Denny, J M., Downing, R. G., Hoffnung, W. I., and Van Atta, W. K., "Charged Particle Radiation Damage in Semiconductors, V: Effect of 1 MeV Electron Bombardment on Solar Cells", Space Technology Labs., Inc., Redondo Beach, California, MR-28, STL-8653-6018-KU-000, February 11, 1963, NAS5-1851, 75 pp.

Denny, J. M., Downing, R. G., Simon, G. W., and Van Atta, W. K., "Charged Particle Radiation Damage in Semiconductors, VI: The Electron Energy Dependence of Radiation Damage in Silicon Solar Cells", Space

Technology Laboratories, Inc., Redondo Beach, California, STL-8653-6019-KU-000, February 13, 1963, NAS5-1851, 24 pp.

Denny, J. M., and Downing, R. G., "Charged Particle Radiation Damage in Semiconductors, VIII: The Electron Energy Dependence of Radiation Damage in Photovoltaic Devices", Space Technology Laboratories, Inc., Redondo Beach, California, STL-8653-6025-KU-000, July 15, 1963, NAS5-1851, 20 pp.

Denny, J. M., and Downing, R. G., "Charged Particle Radiation Damage in Semiconductors, IX: Proton Radiation Damage in Silicon Solar Cells", Space Technology Laboratories, Inc., Redondo Beach, California, STL-8653-6026-KU-000, August 31, 1963, NAS5-1851, 34 pp. Avail: NASA, N65-18050.

De Pangher, J., and Crowther, D. L., "Study of Drift-Field Solar Cells Damaged by Low-Energy Protons", Lockheed Missiles and Space Company, Palo Alto, California, October 15 - November 19, 1965, NAS5-9627, 26 pp, Avail: NASA, N66-14279.

Downing, R. G., TRW Systems, Redondo Beach, California, "Low Energy Proton Degradation in Silicon Solar Cells", Paper presented at Fifth Photovoltaic Specialists Conference, Proceedings held at NASA, Goddard Space Flight Center, Greenbelt, Maryland, October 19, 1965, PIC-SOL-209/6.1, NASA-CR-70169, January, 1966, pp D-7-1 - D-7-11, Avail: NASA, N66-17339.

Downing, R. G., Carter, J. R., Scott, R. E., and Van Atta, W. K., "Charged Particle Radiation Damage in Semiconductors - XIV: Study of Radiation Effects in Lithium Doped Silicon Solar Cells", TRW Systems, Redondo Beach, California, TRW-10971-6014-RO-00, NASA-CR-103788, May 27, 1969, Final Rpt., NAS7-100, 153 pp, Avail: NASA, N69-33422 and NTIS.

Drennan, J. E. and Hamman, D. J., "Space Radiation Damage to Electronic Components and Materials", Battelle Memorial Institute, Columbus Laboratories, Columbus, Ohio, REIC Report No. 39, January 31, 1966, AF 33(616)-1124, 65 pp, Avail: DDC, AD 480010.

Haynes, G. A., and Ellis, W. E., "Effects of 22 MeV Proton and 2.4 MeV Electron Radiation on Boron- and Aluminum- Doped Silicon Solar Cells",

NASA, Langley Research Center, Langley Station, Hampton, Virginia, NASA-TN-D-4407, April, 1968, 66 pp, Avail: NASA, N68-19924.

"Radiation Effects on Lithium P on N Solar Cells", Lockheed-Georgia Co., Marietta, Georgia, LAC-ER-9357, NAS5-10415, 33 pp.

Patterson, J. L., and Miller, W. E., NASA, Langley Research Center, "Protecting Explorer XVI Solar Cells", Astronautics & Aerospace Engineering 1, (9), NASA-RP-115, October, 1963, pp 48-51.

Statler, R. L., U. S. Naval Research Lab., Washington, D. C., "Status of Silicon Solar Cell Radiation Damage", Paper presented at Fifth Photovoltaic Specialists Conference, Proceedings held at NASA, Goddard Space Flight Center, Greenbelt, Maryland, October 19, 1965, PIC-SOL-209/6.1, NASA-CR-70169, January 1966, pp D-2-1 – D-2-20, Avail: NASA, N66-17344.

Statler, R. L., "Radiation Damage in Silicon Solar Cells from 4.6-MeV Proton Bombardment", U. S. Naval Research Laboratory, Washington, D. C., NRL-R-6333, November 15, 1965, Final Rpt., 44 pp.

Weller, J. F., and Statler, R. L., U. S. Naval Research Lab., Washington, D. C., "Low Energy Proton Damage to Solar Cells", Paper presented at the AIEE Summer General Meeting, Toronto, Canada, June 19, 1963, 14 pp, Avail: AIEE as CP-63-1184.

Index

NASA-Langley, 1971 — 9 CR-1872